POLITECNICO DI TORINO
Repository ISTITUZIONALE

Transparent Smart Electromagnetic Skins for Outdoor to Indoor Communications

Original
Transparent Smart Electromagnetic Skins for Outdoor to Indoor Communications / Beccaria, M., Lupinacci, P.F., Massaccesi, A., Pirinoli, P.. - ELETTRONICO. - (2025), pp. 1-3. (19th European Conference on Antennas and Propagation, EuCAP 2025 Stockholm (Swe) 30 March 2025 - 04 April 2025) [10.23919/eucap63536.2025.10999361].

Availability:
This version is available at: 11583/3000907 since: 2025-06-14T12:27:40Z

Publisher:
IEEE

Published
DOI:10.23919/eucap63536.2025.10999361

Terms of use:

This article is made available under terms and conditions as specified in the corresponding bibliographic description in the repository

Publisher copyright
IEEE postprint/Author's Accepted Manuscript

©2025 IEEE. Personal use of this material is permitted. Permission from IEEE must be obtained for all other uses, in any current or future media, including reprinting/republishing this material for advertising or promotional purposes, creating new collecting works, for resale or lists, or reuse of any copyrighted component of this work in other works.

(Article begins on next page)

09 November 2026

Transparent Smart Electromagnetic Skins for Outdoor to Indoor Communications

M. Beccaria, P.F. Lupinacci, A. Massaccesi and P. Pirinoli
Department of Electronics and Telecommunications, DET
Politecnico di Torino
Turin, Italy
michele.beccaria@polito.it, andrea.massaccesi@polito.it, paola.pirinoli@polito.it

***Abstract*—In this communication, preliminary results on the design of a passive, transparent, Smart Electromagnetic Skin (SES) for outdoor-to-indoor (O2I) communications are presented. Contrary to what is already available in literature, here a dielectric-only configuration is proposed, in order to avoid the presence of metallizations that can reduce the transparency. Moreover, a glass layer is directly introduced in the unit cell, to take into account the presence of the window. Different configurations have been designed and numerically analyzed: the obtained results demonstrate the feasibility of the proposed solution and its effectiveness.**

***Index Terms*—5G, 6G, Passive Smart Electromagnetic Skins, Transmitarrays, 3D-Printing, mmWave communications.**

I. Introduction

To meet all the needs of future intelligent and fully integrated automated systems, the next generations of communication networks are demanded to guarantee high performance, in terms of fast data transfer rates, wide bandwidth, better coverage and almost-zero latency. These goals can be achieved using mm-waves or sub-THz frequency bands, that present several advantages, but also suffer from some limitations as higher free space loss, higher building penetration loss, and strong interaction with obstacles along the propagation path. The straightforward solution to overcome these disadvantages would be the introduction of further Base Stations (BSs), but this choice would have a negative impact on the complexity and cost of the network as well as it would contribute to increase the power consumption and the electromagnetic pollution. Recently, the use of the environment in which the propagation occurs, as a further degree of freedom of the communication system has been exploited as a possible solution to enhance its performance. The design of a "Smart Electromagnetic Environment (SEE)" is possible thanks to the introduction of several active and passive devices that allow reaching blind spots or covering desired areas without increasing the number of base stations [1] - [3]. Among them, there are Smart Electromagnetic Skins (SESs), i.e. thin surfaces designed to re-direct the incident field in the desired direction [4] - [9]. In the applications discussed in the past years, they have been mainly considered as reflecting surfaces, while recently, the interest for the possibility to enhance the Outdoor-to-Indoor (O2I) propagation efficiency using transmitting smart skins is increasing [10]. In fact, the signal degradation due to building penetration losses, that can be also of the order of 40 dB at mm-Wave frequencies [10], can hinder the establishment of an O2I link in most practical scenarios. To overcome this signal degradation, the idea is to design a passive, optically transparent SES integrated into the glass of the windows to improve the connection between a base station and the indoor terminals, minimally affecting the passage of light and the visibility.

The problem of designing transparent planar surfaces working in transmitting mode has already been addressed and some results are available in literature. In [11], [12] the design of an optically transparent transmitarray (TA) is carried out, but its integration with the window is not considered. In [10] the glass is used as a (multi-)layer structure, separating two thin film layers, where a conductive pattern is printed. Thanks to the well-established experience in designing dielectric-only antennas [13]- [15], generally realized with Additive Manufacturing (AM) techniques, the authors investigate the possibility to design a totally different and innovative configuration, consisting in a dielectric-only, transparent smart skin integrated with the window. In this framework, an innovative, 2-layer Unit Cell (UC) having resonant size at the design frequency and including a glass layer is first introduced; then its effectiveness is tested through the design and the numerical characterization of both a transmitarray and a smart skin. The obtained results are promising, and prove the feasibility of the proposed solution.

II. Unit Cell Design

As already introduced, the idea is that of designing an innovative unit cell consisting in a layer of glass, to take into account the presence of the window, plus a layer made with a transparent dielectric material. The size of the UC is 5.55 mm, corresponding to $\lambda_0/2$ at the working frequency $f_0 = 27\,\text{GHz}$.

The UC structure is sketched in the inset of Fig. 1a. The glass layer is characterized by relative permittivity $\varepsilon_r = 6.5$, loss tangent $\tan_\delta = 0.024$, as determined experimentally, and thickness $H_g = 6\,\text{mm}$ while for the dielectric layer, values of $\varepsilon_r = 2.7$, $\tan_\delta = 0.01$ and height $H = 16\,\text{mm}$ have been considered. The dielectric block presents a central square hole, whose size d is used to control the behaviour of the UC. Note that the adopted value for H represents a compromise between the need of maximizing the range of variation for the phase of the transmission coefficient S_{21} and the minimization of the unit cell thickness.

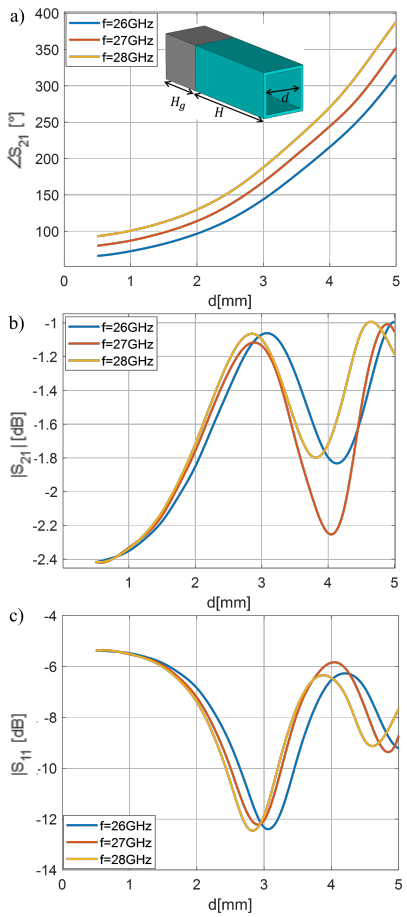

Fig. 1. Phase (a) and magnitude (b) of the transmission coefficient $\angle S_{21}$. Magnitude of the reflection coefficient S_{11} (c). Inset: unit cell structure.

The variation of both the phase and amplitude of S_{21} and of the amplitude of S_{11} as a function of d, and for three different frequencies in the considered band is plotted in Figs. 1a-1c. As it appears, the phase of S_{21} has a almost linear and smooth variation over a range of about 270°, while $|S_{21}|$ is no lower than -2.4 dB and $|S_{21}|$ never higher than -5 dB at all the three considered frequencies. These curves are computed under the assumption of normal incidence of the impinging field.

III. TA Design

Transmitarrays [16]- [19] are good candidates as benchmark structures to test the effectiveness of transmitting unit cells and therefore the considered UC has been assessed through the design of a TA. The considered geometry is sketched in the inset of Fig. 2: the aperture is circular, with diameter $D = 12\lambda_0$, while the feed is the circular horn introduced in [20], [21], whose radiation pattern can be modeled as a $cos^{q_f}(\theta)$ function with $q_f = 12.5$ and it is located at a focal distance from the TA surface of $0.9D$. The TA is designed to radiate a pencil beam in the broadside direction. Note that the glass layer is located internally, on the side of the feed, since the TA anticipates the structure of the SES, mounted on the indoor side of the window.

The numerical analysis of the antenna has been performed using the commercial software CST Microwave Studio. In Fig. 2a, the normalized radiation patterns computed at f_0 in the two principal planes are reported. As it can be seen a well-defined pencil beam radiating in the broadside direction is achieved, with Side Lobe Level (SLL) of -16 dB in the E-plane and -23 dB in the H-plane. The variation of the gain versus

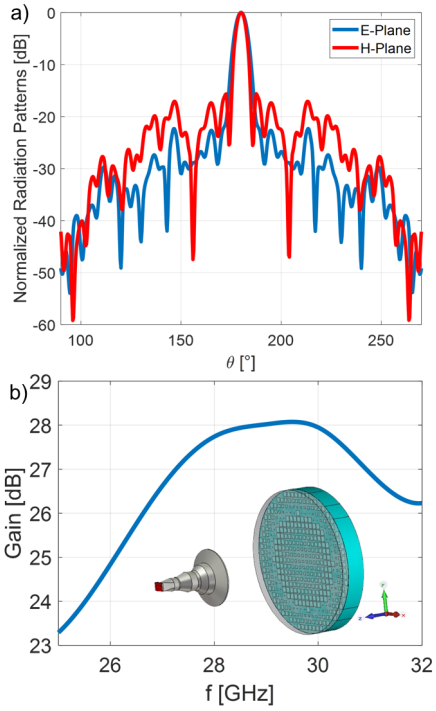

Fig. 2. a) Normalized E- and H- planes radiation patterns. b) Variation of the Gain vs frequency. Inset: sketch of the transmitarray layout.

frequency, shown in Fig. 2b, proves that a 1-dB bandwidth of approximately 14% is obtained. The aperture efficiency is about 39% at 27 GHz.

IV. SES design

In view of the encouraging results obtained by the analysis of the TA, a smart skin has been designed using the same unit cell. The considered structure is rectangular, measures 172.2 $mm \times 222.2$ mm and is discretized with 31×40 unit cells. The plane wave that models the incident field impinges orthogonally on the smart skin, while the desired pointing direction for the transmitted field is identified by $\vartheta_{max} = 160°, \varphi_{max} = 0°$ in the adopted reference system. With the aforementioned specifications, the phase delay that must be compensated by the smart skin in order to produce the desired beam has been computed and is shown in Fig. 3a.

The corresponding layout of the resulting SES is sketched in Fig. 3b, with overlapped the 3D-pattern of the transmitted field, expressed in terms of the Radar Cross Section (RCS) at 27 GHz, obtained through a full-wave simulation using CST Microwave Studio. Finally, in Fig. 4 the behviour of the RCS evaluated at 27 GHz in the two principal planes is reported. The well-defined and focused main beam in the given pointing direction confirms the effectiveness of the SES design. On the other hand, from the pattern in the E-plane the presence of a back lobe lower than the main beam of approximately 6

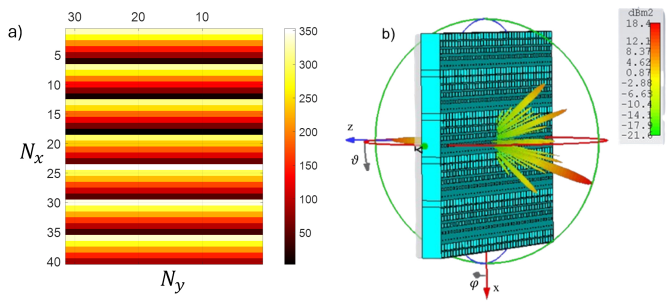

Fig. 3. a) Required phase distribution map. b) Sketch of the SES layout with the 3D-pattern of the transmitted field at the design frequency of 27 GHz.

dB, point outs that a further optimization of the unit cell is required to reduce $|S_{11}|$.

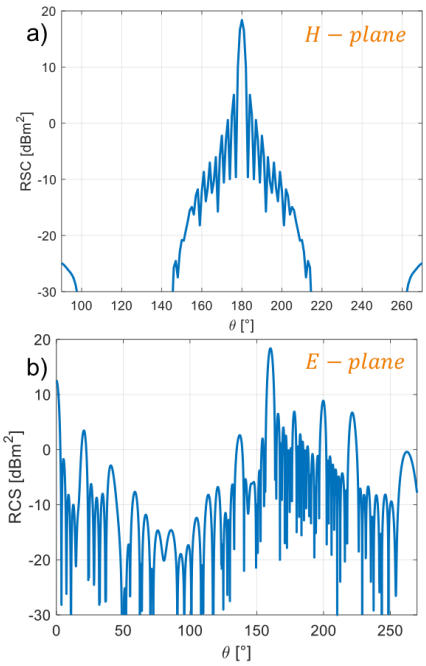

Fig. 4. RCS behaviour at 27 GHz, in the two principal planes. a)H-plane. b) E-plane.

V. Conclusions

In this communication, the preliminary results of the design and analysis of optically transparent transmitting surfaces are summarized: they confirm that the proposed solution is a good candidate for the realization of a passive SES, capable of operating in an urban scenario within the framework of O2I communications. Nevertheless, some improvements in the adopted UC are necessary especially for reducing the back radiation. At the time of the conference, further results about other SESs, designed using an optimized UC, will be presented.

Acknowledgement

This work was supported by the European Union - Next Generation EU under the Italian National Recovery and Resilience Plan (NRRP), Mission 4, Component 2, Investment 1.3, CUP E13C22001870001, partnership on "Telecommunications of the Future" (PE00000001 - program "RESTART")

References

[1] S. Kisseleff, W. A. Martins, H. Al-Hraishawi, S. Chatzinotas and B. Ottersten, "Reconfigurable Intelligent Surfaces for Smart Cities: Research Challenges and Opportunities," in *IEEE Open Journal of the Communications Society*, vol. 1, pp. 1781-1797, 2020.

[2] R. Flamini *et al.*, "Toward a Heterogeneous Smart Electromagnetic Environment for Millimeter-Wave Communications: An Industrial Viewpoint," in *IEEE Trans. on Antennas Propag.*, vol. 70, no. 10, pp. 8898-8910, Oct. 2022.

[3] W. Luo, T. Yan, A. Xuan, Y. Zhong and X. Zhao, "Adaptive Smart Radio Environment (ASRE): New Paradigm for Wireless Communication Networks," in *IEEE Access*, vol. 12, pp. 12437-12445, 2024.

[4] E. Basar *et al.*, "Wireless Communications Through Reconfigurable Intelligent Surfaces," in *IEEE Access*, vol. 7, pp. 116753-116773, 2019.

[5] E. Martinez-de-Rioja *et al.*, "Passive intelligent reflecting surfaces based on reflectarray panels to enhance 5G millimeter-wave coverage." *Int. J. Microw. Wirel. Tech.*, vol. 15, pp. 1-12, 2022.

[6] M. Salucci *et al.*, "A Multihop Strategy for the Planning of EM Skins in a Smart Electromagnetic Environment," in *IEEE Transactions on Antennas and Propagation*, vol. 71, no. 3, pp. 2758-2767, March 2023.

[7] A. Freni, M. Beccaria, A. Mazzinghi, A. Massaccesi, P. Pirinoli, "Low-Profile and Low-Visual Impact Smart Electromagnetic Curved Passive Skins for Enhancing Connectivity in Urban Scenarios," *Electronics*, vol. 12, no. 21, p. 4491, Nov. 2023.

[8] M. Beccaria, A. Freni, A. Mazzinghi, A. Massaccesi and P. Pirinoli, "Curved Electromagnetic Skins for Urban Scenarios," *2024 18th European Conference on Antennas and Propagation (EuCAP)*, Glasgow, United Kingdom, 2024, pp. 1-5.

[9] M. Beccaria, A. Mazzinghi, A. Freni and P. Pirinoli, "Beam Scanning Capability of Passive Smart Eelctromagnetic Skins," *2024 IEEE INC-USNC-URSI Radio Science Meeting (Joint with AP-S Symposium)*, Florence, Italy, 2024, pp. 438-438.

[10] G. Oliveri, F. Zardi, G. Gottardi, A. Massa "Optically-Transparent EM Skins for Outdoor-to-Indoor mm-Wave Wireless Communications," *IEEE Access*, vol. 12, pp. 65178-65191, 2024.

[11] G. Liu, E. M. Cruz, K. Pham, D. G. Ovejero and R. Sauleau, "Low Scan Loss Bifocal Ka-band Transparent Transmitarray Antenna," *2018 IEEE International Symposium on Antennas and Propagation & USNC/URSI National Radio Science Meeting*, Boston, MA, USA, 2018, pp. 1449-1450.

[12] G. Liu *et al.*, "A Millimeter-Wave Multibeam Transparent Transmitarray Antenna at Ka-Band," *IEEE Antennas and Wireless Propagation Letters*, vol. 18, no. 4, pp. 631-635, April 2019.

[13] A. Massaccesi *et al.*, "3D-Printable Dielectric Transmitarray With Enhanced Bandwidth at Millimeter-Waves," in *IEEE Access*, vol. 6, pp. 46407-46418, 2018.

[14] A. Massaccesi *et al.*, "Three-Dimensional-Printed Wideband Perforated Dielectric-Only Reflectarray in Ka-Band," in *IEEE Transactions on Antennas and Propagation*, vol. 71, no. 10, pp. 7848-7859, Oct. 2023.

[15] A. Massaccesi *et al.*, "3D-printed wideband reflectarray antennas with mechanical beam-steering," *International Journal of Microwave and Wireless Technologies*, vol. 16, no. 1, pp. 21–29, 2024.

[16] A. H. Abdelrahman, F. Yang, and A. Z. Elsherbeni. "Analysis and Design of Transmitarray Antennas." Morgan & Claypool Publishers, 2017.

[17] M. Beccaria, P. Pirinoli and F. Yang, "Preliminary results on Conformal Transmitarray Antennas," *2018 IEEE International Symposium on Antennas and Propagation & USNC/URSI National Radio Science Meeting*, Boston, MA, USA, 2018, pp. 265-266.

[18] M. Beccaria, A. Massaccesi, P. Pirinoli and L. H. Manh, "Multibeam Transmitarrays for 5G Antenna Systems," *2018 IEEE Seventh International Conference on Communications and Electronics (ICCE)*, Hue, Vietnam, 2018, pp. 217-221.

[19] J. R. Reis, M. Vala and R. F. S. Caldeirinha, "Review paper on transmitarray antennas", *IEEE Access*, vol. 7, pp. 94171-94188, 2019.

[20] M. Beccaria *et al.*, "Feed system optimization for convex conformal reflectarray antennas," *2017 IEEE International Symposium on Antennas and Propagation & USNC/URSI National Radio Science Meeting*, San Diego, CA, USA, 2017, pp. 1187-1188.

[21] M. Beccaria *et al.*,"Enhanced Efficiency and Reduced Side Lobe Level Convex Conformal Reflectarray," *Applied Sciences*. 2021; 11(21): 9893.